

A Novel 31-Channel Imaging Grid Coil

Wolfgang Loew¹, Nathan Lamba², Randy Giaquinto¹, Matthew Lanier¹, Lacey Sickinger¹, Brynne Williams¹, Christopher Ireland¹, Yu Li¹, and Charles Dumoulin¹
¹Imaging Research Center, Cincinnati Children's Hospital Medical Center, Cincinnati, Ohio, United States, ²Ohio State University, Ohio, United States

Target Audience: RF coil designers and everyone who is interested in novel coil design and image reconstruction.

Purpose: In this abstract we present a novel concept for detecting MR signals. Traditional signal acquisition uses resonant loop coils¹ or other antennas such as dipoles² or coil/dipole combinations³ in high field applications. Typically these structures are assembled into phased arrays^{1,4} to accommodate imaging needs. Construction of high channel-count phased arrays requires a large number of components and an experienced skillset. Matching is required for the each desired anatomy due to the different composition of tissue in the human body. Our approach uses a combination of a non-resonant grid structure and resonant coil elements for signal pick up. The non-resonant structure is inductively coupled to resonant integrated balun coils (IBC)⁵.

A grid with 31 segments and 31 transformers was constructed on a planar circuit board and coupled to 31 IBCs. Network measurements and imaging experiments were performed on phantoms to evaluate the potential of this new approach.

Methods: A rectangular grid was constructed on a 9" x 12" FR4 board using coated 12 AWG magnet wire. Each individual grid segment was 70mm long. 31 segments were arranged to form twelve 70mm x 70mm squares. Each segment was constructed with a 19 mm loop in its center which was inductively coupled to an Integrated Balun Coil (IBC). Each IBC was attached to an independent receive channel of the MR system (Figure 1). Although the grid is non-resonant, all

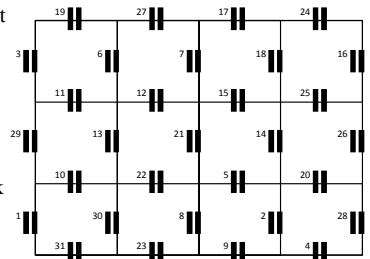


Figure 1: 31 segment grid with 1:1 transformers used to detect MR signals in each segment.

IBCs were matched and tuned to the Larmor frequency. High-value chip capacitors were integrated into the grid at segment intersections to prevent gradient-induced eddy currents in the structure.

The inductive loop on each segment and the IBCs were constructed with the same diameter (19 mm), and fastened to each other with a nylon 5/16-18 screw and nut. The spacing between the loop and IBC was fixed with two nylon washers (each between 0.05" and 0.07" thick). The inductive loop and IBCs were placed 9 mm above the FR4 board. To minimize direct MR signal pickup through the resonant coils, all segment loops and IBCs were placed in the xy plane so the main magnetic field vector, B_0 , was oriented axially through the loop. Lexan support blocks were added to each IBC feed board to enhance dimensional stability. The prototype coil is shown in Figure 2.

IBC elements were connected to preamps at a distance of $\lambda/2$. For the prototype setup no cable baluns were used. The S-Parameter Matrix for this setup was acquired with a Rhode & Schwarz ZNC3 Vector Network Analyzer with and without loading.

Imaging experiments were performed on a Philips 3T Achieva™ (Philips Healthcare, Best, Netherlands) scanner. A collection of fruit was imaged with a T2 weighted turbo spin echo sequence (90° flip angle TR:8001msec, TE:10msec, Matrix 400 x 400, resolution 0.68mm x 0.68mm x 3mm, slice thickness 3mm, FOV:270mm x 270mm, 1 average, CLEAR enabled), and a T2 weighted gradient echo sequence (30° flip angle TR:8.6msec, TE:4.2msec, Matrix 320 x 320, resolution 0.84mm x 0.84mm x 3mm, slice thickness 3mm, FOV:270mm x 270mm, 1 average, CLEAR enabled).

Results and Discussion: Network analyzer measurements with a variety of loads showed that the grid coil is insensitive to loading. This insensitivity is due to the size, orientation and distance of the resonant pickup coils from the load. In addition, S-Parameters did not change significantly between different loads or no load. Individual element tuning and matching was on average -17 dB and the isolation between channels was better than -20 dB for 94.6% of the matrix for all loading conditions. The highest coupling was measured with -13.3dB.

A 3dB transfer loss was measured between the grid transformer and IBC. However, imaging experiments showed that even with a non-resonant structure, high quality imaging was possible. The SNR of the grid was observed to be about half that of conventional resonant coil designs. Use of the coil for accelerated imaging was straightforward.

Unlike prior work, the grid coil is not optimized for ideal current patterns⁶. Indeed, an attractive aspect of the approach is that the induced currents find their own way through the grid without being constrained to discrete loops. An

additional advantage of the novel grid approach is that the individual MR signals collected in each segment can be retrospectively combined to form synthetic (or virtual) surface coils with arbitrary geometries. These synthetic surface coils can be independently optimized for detection of MR signals in each region of the image. The approach is not limited to the rectangular grid shown above, but can be readily extended to other grid geometries including triangular, hexagonal or even arbitrary networks of segments. These and other characteristics of this novel approach are being investigated, and performance comparisons of SNR and g-factors are being made with respect with conventional arrays.

References:

1. Roemer P B, Edelstein W A, et al. The NMR Phased Array. MRM 16:192-225 (1990).
2. Rennings A, et al. A Full-Wavelength Dipole RF Coil Element for 7 T MRI with Maximized Longitudinal FOV and Two-Peak SAR Distribution. ISMRM 2010: 3813.
3. Wiggins C J, et al. Combining Cylindrically Mounted Dipoles with Loops on a Transverse Plane for Better Head Coverage in Parallel Transmission, ISMRM 2012: 2783.
4. Wiggins G C, et al. 32-Channel 3 Tesla Receive-Only Phased-Array Head Coil With Soccer-Ball Element Geometry. MRM 56:216-223 (2006).
5. Loew W, Giaquinto R, et al. An 8-Channel Integrated Balun Coil for Small Anatomical Features. ISMRM 2014: 1323.
6. Lattanzi R, et al. Ideal current patterns yielding optimal signal-to-noise ratio and specific absorption rate in magnetic resonance imaging: Computational methods and physical insights. MRM 68 (1): 286-304 (2012).

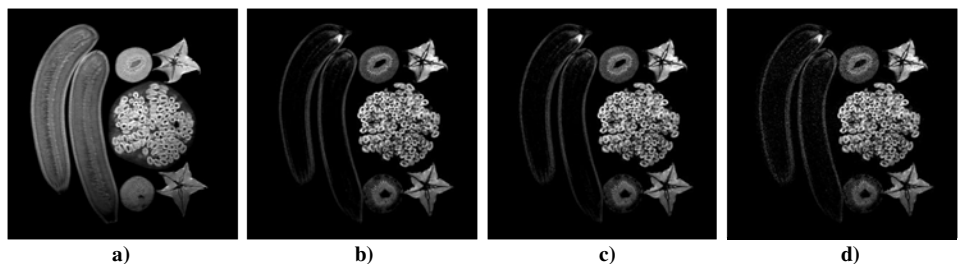


Figure 4: Coronal images of bananas, kiwis, star fruit and a pomegranate acquired with a) T2 weighted turbo spin echo, b) with a T2w gradient echo, c) accelerated 2x2, and d) accelerated 4x2.

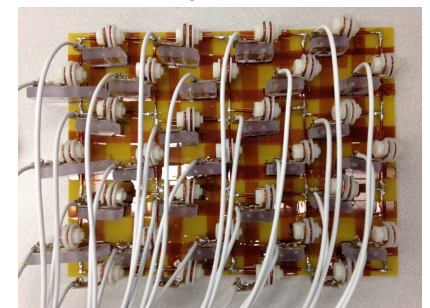


Figure 2: 31-channel grid using integrated balun coils.

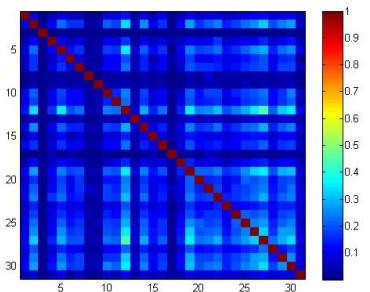


Figure 3: Normalized noise correlation matrix.